Numerical Investigation of Factors Causing Near-Surface Metamorphism

Andrew E. Slaughter* and Edward E. Adams
Department of Civil Engineering, Montana State University, Bozeman, MT

ABSTRACT: Buried layers of surface hoar or near-surface facets within the snowpack are well known to be the culprit in a majority of avalanches. Near-surface metamorphism has been the topic of a multitude of field, laboratory, and analytical investigations. Analytically, a variety of models are capable of reasonably modeling temperature in the snowpack. Using a computationally efficient 1-D thermal model, the SOBOL method of sensitivity analysis was implemented to exploit modern computational resources. To the authors' knowledge, this has yet to be done for specific metamorphic processes. The resulting sensitivity indices quantify the relative importance of each input as well as the importance of the interaction between inputs. The sensitivity results for radiation-recrystallization confirm the conceptual understanding of the process indicating that thermal conductivity, albedo, and long- and short-wave radiation are the most influential, with the thermal conductivity being highly interactive. Surface hoar was heavily dependent on long-wave radiation and to some extent wind speed, air temperature, and humidity, but revealed little interaction between these terms. Finally, the optimum environmental and snow conditions conducive to radiation-recrystallization and surface hoar are quantified statistically. These numerically determined conditions compared well with recorded field data of radiation recrystallization and to a lesser extent with recorded surface hoar events. The research presented here is intended to be a tool among many for assessing near-surface metamorphism as well as designing additional experimentation.

KEYWORDS: Facets, Surface Hoar, Radiation-Recrystallization, Numerical Analysis, Monte Carlo, Sensitivity

1 INTRODUCTION

Near-surface facets and surface hoar are two of the most common weak-layers leading to slab avalanches (Schweizer and Lutschg, 2001). Research discussing the conditions necessary for producing these layers is widespread and includes field studies (Colbeck and Jamieson, 2006; McCabe et al., 2008), laboratory investigations (Morstad et al., 2007), and studies linking the two (Slaughter et al., in press). Additionally, computer models continue to increase in accuracy for predicting weak-layers and stability (Lehning et al., 2004) as well as model the snowpack spatially (Staples et al., 2006; Adams et al., 2009).

As computer models become more prevalent it is evermore appropriate to use the models as a tool for gaining additional information about the snowpack behavior, in this case the environmental conditions leading to radiation-recrystallization and surface hoar formation. Using computational statistical methods along with a 1-D snowpack model it is possible to explore an enormous range of environmental inputs and quantify which inputs are most critical, how they interact, and what conditions may be optimal for facet and surface hoar formation.

* *Corresponding author address:* Andrew E. Slaughter, 205 Cobleigh Hall, Montana State University, Bozeman, MT 59717; tel: 406-994-2293; fax: 406-994-6105; email: andrewEslaughter@gmail.com

2 METHODS

Two statistical approaches were utilized: sensitivity analysis and Monte Carlo simulations. The sensitivity analysis quantifies how much the variance of each input contributes to the variance of the model output. Monte Carlo analysis allows the input resulting in a specific output to be separated establishing an optimum range of conditions for the desired output. Both methods require hundreds of thousands of model evaluations, as such, a computationally efficient model is required.

2.1 Thermal Model

The 1-D model originally implemented by Morstad et al. (2007) was utilized for all analysis presented. During model evaluations all parameters remained constant, except short-wave radiation which was varied as a sine-wave, the 11 input parameters explored are listed in Table 1. The model was run for 10 hours. All inputs were allowed to vary independently.

The analysis requires that each input be fitted to a continuous distribution function. The first five input parameters where assigned uniform distributions based on data published by Armstrong and Brun (2008) as summarized in Table 1. The remaining six parameters where assigned distributions associated with recorded field data. The field data was acquired from north and south facing weather stations at the Yellowstone Club over the 07/08 and 08/09 seasons. Details of these stations may be found in Slaughter et al. (in press). Two distribution sets were constructed, a daylight and night set, where the daylight

Table 1. Details of thermal model input parameters including the upper and lower limits used for sensitivity analysis and Monte Carlo simulations.

i	*Sym.*	*Units*	*Name [min,max]*
1	ρ	kg/m^3	snow density [50,500]
2	k	W/(m K)	thermal conductivity [0.01,0.7]
3	C_p	kJ/(kg K)	specific heat [1795,2115]
4	α		albedo [0.4,0.95]
5	κ	m^{-1}	extinction coefficient [40,200]
6	T_s^{int}	°C	initial snow temperature [-40,0]
7	LW	W/m^2	incoming long-wave rad. [100,600]
8	SW	W/m^2	incoming short-wave rad. [50,800]
9	V_w	m/s	wind speed [0,10]
10	T_a	°C	air temperature [-30,10]
11	RH	%	relative humidity [0,100]

set based on the south weather station was used for assessing radiation-recrystallization and data from the north station during the night was used for surface hoar assessment. The distributions were limited by the min/max values listed in Table 1. The distributions are based on mean daily/nightly values of short-wave and long-wave radiation, wind speed, air temperature, and relative humidity. The initial snow temperature was assigned a value at sunrise for the daylight set and sunset for the night set. Table 2 summarizes these distribution sets, which were fit using EasyFit 5.0 (Mathwave Technologies).

Three outputs were examined: temperature gradient between the surface and a depth of 5 cm, a "knee" temperature gradient, and mass flux at the snow surface. The "knee" output is characteristic of what would likely form due to solar penetration and surface radiative cooling, as shown in the schematic of Figure 1, which is typically associated with radiation-recrystallization (Birkeland, 1998). In this case, the gradient was calculated between the surface and the inflection point. Both gradients outputs were calculated using the south, daylight input. Mass flux was computed using the latent heat flux value computed by the thermal model using the north, night data set. It is important to note that the results presented in this work only considered the resulting conditions that are understood to form near-surface facets and surface hoar, no micro-structural analysis is incorporated into the model.

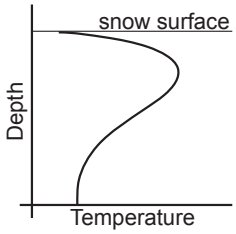

Figure 1. Schematic showing the "knee" temperature profile.

2.2 Sensitivity Analysis

The extended SOBOL variance-based sensitivity method (Saltelli, 2002) quantifies the contribution of the variance of each input parameter (see Table 1) and the interactions between input parameters to the total variance of the model output. The SOBOL method was performed using the thermal model to compute output based on the input parameters and associated statistical distributions, using a sampling size of 10,000 replicates. The 90% confidence intervals were calculated using bootstrap BCa method (Efron and Tibshirani, 1993) with 10,000 re-samplings. The results discussed include four terms: the first-order index S_i gives the contribution of the i^{th} input parameter; the second-order index $S_{i,j}$ gives the contribution due to interaction between i^{th} and j^{th} terms; a higher-order index S_h, which includes all interactions greater than second-order; and the total-effect index S_i^T provides the contribution of the i^{th} parameter and all associated interactions to the k^{th} order (e.g. $S_1^T = S_1 + S_{1,2} + S_{1,3} + \ldots$), where k is the number of input factors. The i and j subscripts refer to the variable numbers in Table 1.

Table 2. Continuous distributions functions for environmental input parameters. The parameters (a,b,c) are order as defined in the EasyFit 5.0 manual (EasyFit 5.0, 2009)(gev = generalized extreme value; gp = generalize pareto; logn = lognormal).

	South (daylight)				*North (night)*			
	type	*a*	*b*	*c*	*type*	*a*	*b*	*c*
T_s^{int}	gev	-0.39	5.80	-16.34	gev	-0.40	5.19	-13.15
LW	gev	-0.09	63.62	288.0	gev	0.07	35.84	236.8
SW	gp	-0.89	575.8	39.09				
V_w	logn	0.52	0.33	0.00	gev	-0.17	0.35	1.02
T_a	gev	-0.24	4.47	-8.19	gev	-0.41	4.68	-10.11
RH	gev	-0.66	15.92	60.43	gev	-0.80	11.26	70.90

2.3 Monte Carlo Analysis

The SOBOL method quantifies the significance of the input, but does not yield results linking inputs that lead to a certain output. Thus, Monte Carlo simulations (Press et al., 1986) were utilized to further quantify the conditions by separating the portion the critical input parameters leading to a specific output, e.g. what levels of long-wave radiation correspond to high temperature gradients at the surface. The input factors must be defined by a continuous probability distribution. Next, these distributions are sampled randomly (125,000 times here) and the thermal model executed for each sampling. Finally, the inputs are parsed to include only the values corresponding to a particular output quantity.

3 RESULTS

3.1 Near-Surface Facets (Temperature Gradient)

The resulting total-effect indices for the temperature gradient in the top 5 cm are presented in Figure 2, which show that ρ, k, κ, T_s^{int}, LW, and T_a are the most influential terms. For the two largest contributors, T_s^{int} and LW, the total-effect results are broken down into first-, second-, and higher-order terms to determine the interactions that are important (Figures 3a and 3b). In both cases, a majority of the sensitivity is due to the variance of the input parameter alone (S_6 and S_7 respectively); however,

each interacts with k. Examining k in a similar manner, as shown in Figure 3c, indicates that a majority of this term is due to interactions. Thus, k is only significant when working congruently with other terms.

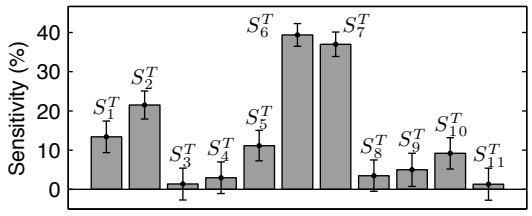

Figure 2. Total-effect indices using daylight evaluations for the mean temperature gradient between the surface and 5 cm depth; the subscripts refer the the input parameters listed in Table 1.

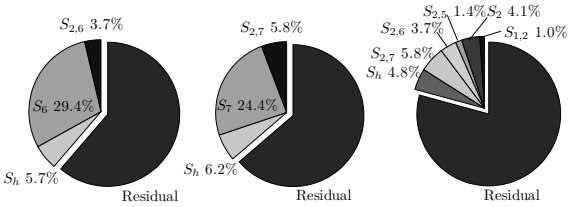

(a) T_s^{int} (b) LW (c) k

Figure 3. Break-down of total-effect index components for (a) LW, (b) T_s^{int}, and (c) k; residual refers to all components not associated with the index and the subscripts correspond to values in Table 1.

Using the mean temperature gradient only yields a broad examination into the sensitivity, a more detailed result may be gained by examining the sensitivity as a function of time, as in Figure 4. As expected, when time progresses κ becomes more intense while LW decreases, the trend reverses towards the end of the day. Examining the sensitivity at mid-day (5 hr) shows that during peak SW the most influential parameters shift to ρ, k, and κ, while LW is diminished.

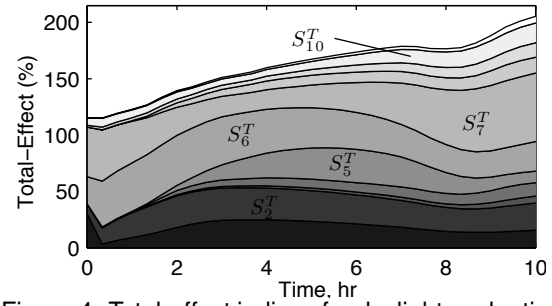

Figure 4. Total-effect indices for daylight evaluations of south input data over the 10 hours of the experiment; the indices are stacked bottom to top as number in Table 1.

The results thus far are for temperature gradient in general, this may be refined by only considering gradients that form a characteristic "knee"(i.e.

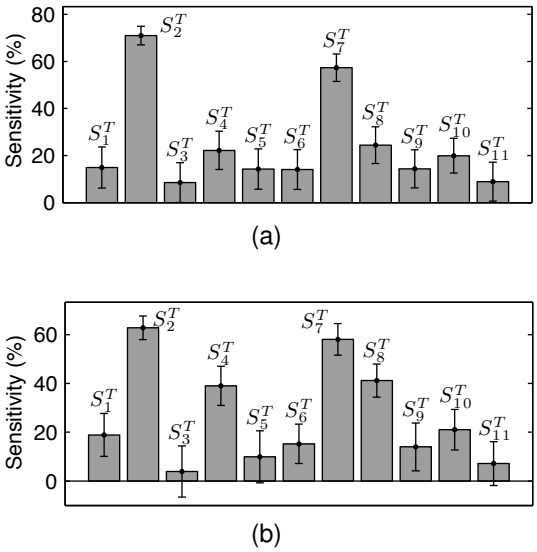

Figure 5. Total-effect indices based on "knee" temperature gradient of (a) the daily mean gradient and (b) the gradient at mid-day.

radiation-recrystallization). In this case, as indicated in Figure 5a, the critical components are k and LW. However; examining the results at mid-day indicate (Figure 5b) that α and SW also are critical components and contribute significantly to the variance of the "knee" gradient.

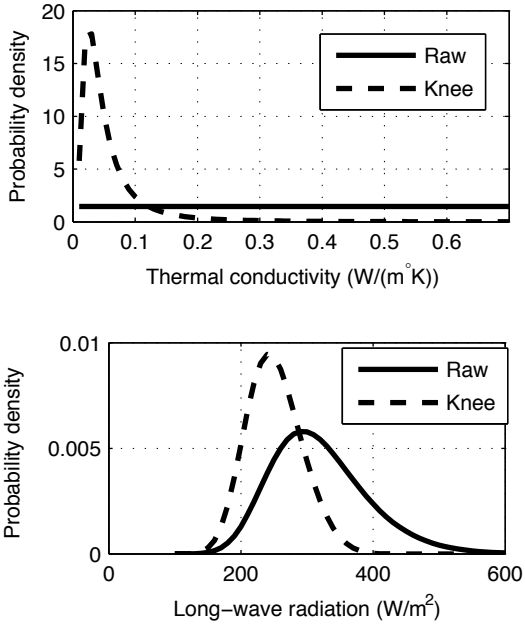

Figure 6. Probability distributions for data input (raw) and input resulting in a temperature gradient "knee" of 200–500 °C/m for input k and LW input parameters at mid-day.

The Monte Carlo analysis allows for the critical parameters to be further scrutinized. Figure 6 are graphs of the input probability density distribution (PDF) and the PDF of input values for k and LW that lead to the formation of a "knee" temperature gradient of 200–500 °C/m for a duration of at least

5 hours (17.3% of model evaluations resulted in this scenario). This gradient range is consistent with recent radiation-recrystallization formation data (Morstad et al., 2007; Slaughter et al., in press). The resulting PDF's for the four critical parameters were fit to generalized extreme value distributions, the parameters are provided in Table 3a.

Table 3. Parameters for the generalized extreme value distributions fitted to the input parameters that lead to (a) "knee" temperature gradients of 200–500 °C/m and (b) mass flux of 3.6–4.4 gm/m^2/hr.

(a)

	a	b	c
k	0.401	0.021	0.032
α	-0.531	0.165	0.659
LW	-0.181	37.9	233
SW	-0.157	151	260

(b)

	a	b	c
LW	-0.187	20.4	215
V_w	-0.153	0.327	1.03
T_a	-0.378	3.03	-6.73
RH	-0.759	7.84	74.6

3.2 Surface Hoar (Mass Flux)

The sensitivity analysis for the mass flux reveals that LW is overwhelmingly the most critical component, with V_w, T_a, and RH contributing to a small extent (see Figure 7). Little interaction occurred between these factors and when plotted over time the system becomes steady-state within about two hours, which is expected given the model setup.

The Monte Carlo analysis examines input parameters that resulted in mass flux rates of 3.6–4.4 gm/m^2/hr; the lower end of the range corresponds to the rate used by Colbeck et al. (2008) and the upper being four times that rate. 23.6% of the data resulted in mean mass flux values in this range. The raw LW input values and input associated with the desired output are shown in Figure 8. Again, the four critical components for mass flux were fit to generalized extreme value distributions, the parameters are summarized in Table 3b.

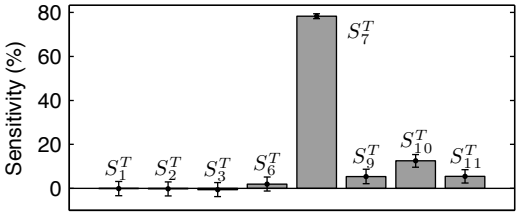

Figure 7. Total-effect indices for the mean mass flux of night evaluations of north input data; the indices refer the the input parameters listed in Table 1.

4 ANALYSIS

The distribution functions defined in Table 3 present a tool for assessing the formation of radiation-recrystallization and surface hoar based on the environmental and snow conditions. Using defined distributions, Table 4 was produced, which is a tabular version of the PDF distributions, it contains the most probable (peak) value and the values that are 75%, 50%, and 25% as probable on either side of the peak.

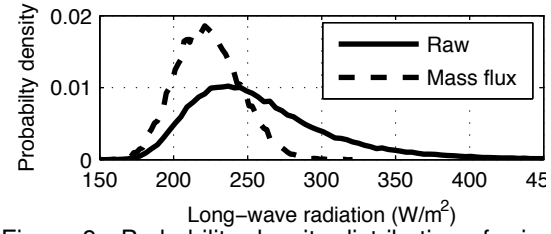

Figure 8. Probability density distributions for input (raw) and input resulting in mass flux onto the snow surface of 3.6–4.4 gm/m^2/hr for incoming long-wave radiation. The parameters (a,b,c) are order as defined in the EasyFit 5.0 manual (EasyFit 5.0, 2009).

Table 4. Probability chart for the critical input parameters for "knee" temperature gradient (unshaded) and mass flux (shaded) favorable for radiation-recrystallization and surface hoar development; units are consistent with Table 1.

	0.25	0.5	0.75	Peak	0.75	0.5	0.25
k	0.014	0.019	0.024	0.038	0.062	0.086	0.13
α	0.51	0.60	0.67	0.79	0.88	0.92	0.94
LW	187	204	217	247	279	300	320
SW	139	195	253	365	499	570	666
LW	190	197	205	221	238	250	261
V_w	0.7	0.8	0.9	1.2	1.5	1.7	1.9
T_a	-11.6	-10.3	-9.2	-7.0	-4.8	-3.7	-2.5
RH	68.1	73.0	76.7	81.7	84.2	84.6	84.6

Slaughter et al. (in press) detailed three days with radiation-recrystallization, the recorded conditions for these three events are included Table 5a. The thermal conductivity was calculated based on recorded density values and the relationship proposed by Sturm et al. (1997). The upper portion of Figure 9 is a graphical representation to where the recorded environmental conditions listed in Table 5a fit into the theoretical ideal conditions of Table 4. For example, the first k from Table 5a is 0.035, which is near the peak value in Table 4, thus in Figure 9 an "X" is place in the k row (y-axis) near the peak value (x-axis). In the case of the three radiation recrystallization events, the recorded data, with one exception, all lie near the most probable conditions indicating the potential for the "knee" temperature gradient to predict the formation of facets.

Table 5b list four days of surface hoar documented during the 2008/2009 season at the north weather station. The data from these events are also presented graphically in the lower portion of Figure 9. The mass flux results do not match up as well as the radiation-recrystallization results: only 50% of the data was near the peak value, indicating that mass flux alone or the simplistic model utilized may not be adequate to predict surface hoar formation.

Table 5. Data recorded from field stations of (a) radiation-recrystallization and (b) surface hoar events.

(a)

	k	α	LW	SW
#1	0.035	0.86	250	292
#2	0.043	0.84	350	250
#3	0.041	0.81	420	300

(b)

	LW	V_w	T_a	RH
#1	262	0.53	-5.7	84
#2	210	1.37	-6.4	61
#3	202	1.35	-6.1	63
#4	175	1.23	-15.	75

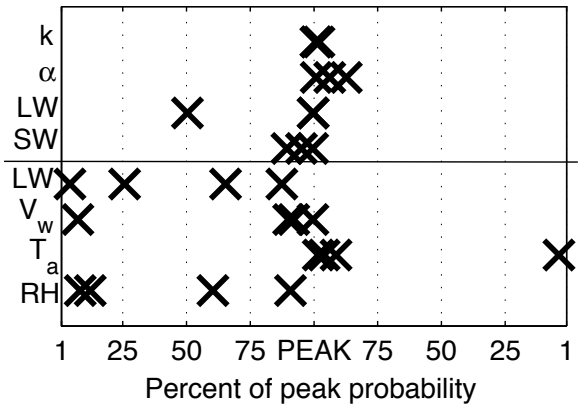

Figure 9. Graphical representation to where the recorded input environmental conditions from field observations (Table 5)of radiation-recrystallization (upper portion) and surface hoar observations (lower portion) fit in the tabulated probabilities of Table 4.

5 CLOSING REMARKS

This research is a small portion of the analysis underway and only scratches the surface of the possibilities for such analysis. However, the results obtained indicate the potential to use purely numerical methods to gain an understanding of the environmental conditions that lead the formation of weak-layers. Future analysis will include layered snowpacks, contaminated layers, and various initial conditions and input data sets that will inevitably expand upon the results presented here. Also, the authors believe that similar analysis should be conducted using more detailed models that include a micro-structural components such as SNOWPACK.

6 ACKNOWLEDGMENTS

Research was conducted at Montana State University's Subzero Science and Engineering Research Facility, which was developed with the National Science Foundation (NSF) Grant #ANT-0521360 and Murdock Charitable Trust. A portion was funded by NSF Grant #EAR-0635977, the NSF GK–12 Program, and grants from the 2000 ISSW and American Avalanche Association.

7 REFERENCES

Adams, E., et al., 2009: Modeling variation of surface hoar and radiation recrystallization across a slope. *International Snow Science Workshop*, Davos, CH.

Armstrong, R. L. and E. Brun, 2008: *Snow and Climate: Physical Processes, Surface Energy Exchange, and Modeling*. Cambridge University Press.

Birkeland, K. W., 1998: Terminology and predominat processes associated with the formation of weak layers of near-surface faceted crystals in the mountain snowpack. *Arctic and Alpine Research*, **30 (2)**, 193–199.

Colbeck, S. and B. Jamieson, 2006: Surface hoar growth from valley clouds. *International Snow Science Workshop*, Telluride, CO.

Colbeck, S., B. Jamieson, and S. Crowe, 2008: An attempt to describe the mechanism of surface hoar growth from valley clouds. *Cold Regions Science and Technology*, **54 (2)**, 83–88.

EasyFit 5.0, 2009: *EasyFit Help Online*. Mathwave Technologies, URL `www.mathwave.com/help/easyfit/index.html`.

Efron, B. and R. J. Tibshirani, 1993: *An introduction to the Boostrap*. Chapman and Hall.

Lehning, M., C. Fierz, B. Brown, and B. Jamieson, 2004: Modeling snow instability with the snow-cover model snowpack. *Annals of Glaciology*, **38 (1)**, 331–338.

McCabe, D., et al., 2008: Near-surface faceting on south aspects in southweast Montana. *International Snow Science Workshop*, Whistler, B.C., 147–154.

Morstad, B., E. Adams, and L. McKittrick, 2007: Experimental and analytical study of radiation-recrystallized near-surface facets in snow. *Cold Regions Science and Technology*, **47 (1-2)**, 90–101.

Press, W. H., B. P. Flannery, S. A. Teukolsky, and W. T. Vetterling, 1986: *Numerical Recipies*. Cambridge University Press.

Saltelli, A., 2002: Making best use of model evaluations to compute sensitivity indices. *Computer Physics Communications*, **145**, 280–297.

Schweizer, J. and M. Lutschg, 2001: Characteristics of human-triggered avalanches. *Cold Regions Science and Technology*, **33**, 147–162.

Slaughter, A., et al., in press: An investigation of radiation-recrystallization coupling laboratory and field studies. *Cold Regions Science and Technology*.

Staples, J., E. Adams, A. Slaughter, and L. McKittrick, 2006: Slope scale modeling of snow surface temperature in topographically complex terrain. *International Snow Science Workshop*, Telluride, CO, 806–814.

Sturm, M., J. Holmgren, and M. König, 1997: The thermal conductivity of seasonal snow. *Journal of Glaciology*, **43 (143)**, 26–41.